

# Applications of surface metrology in firearm identification

X Zheng<sup>1</sup>, J Soons<sup>1</sup>, T V Vorburger<sup>1</sup>, J Song<sup>1</sup>, T Renegar<sup>1</sup>  
and R Thompson<sup>2</sup>

<sup>1</sup> Semiconductor & Dimensional Metrology Division, National Institute of Standards and Technology,  
100 Bureau Drive, Gaithersburg, MD 20899, USA

<sup>2</sup> Law Enforcement Standards Office, National Institute of Standards and Technology, 100 Bureau Drive,  
Gaithersburg, MD 20899, USA

E-mail: [alan.zheng@nist.gov](mailto:alan.zheng@nist.gov)

Received 21 August 2013, revised 8 November 2013

Accepted for publication 2 December 2013

Published 8 January 2014

## Abstract

Surface metrology is commonly used to characterize functional engineering surfaces. The technologies developed offer opportunities to improve forensic toolmark identification. Toolmarks are created when a hard surface, the tool, comes into contact with a softer surface and causes plastic deformation. Toolmarks are commonly found on fired bullets and cartridge cases. Trained firearms examiners use these toolmarks to link an evidence bullet or cartridge case to a specific firearm, which can lead to a criminal conviction. Currently, identification is typically based on qualitative visual comparison by a trained examiner using a comparison microscope. In 2009, a report by the National Academies called this method into question. Amongst other issues, they questioned the objectivity of visual toolmark identification by firearms examiners. The National Academies recommended the development of objective toolmark identification criteria and confidence limits. The National Institute of Standards and Technology (NIST) have applied its experience in surface metrology to develop objective identification criteria, measurement methods, and reference artefacts for toolmark identification. NIST developed the Standard Reference Material SRM 2460 standard bullet and SRM 2461 standard cartridge case to facilitate quality control and traceability of identifications performed in crime laboratories. Objectivity is improved through measurement of surface topography and application of unambiguous surface similarity metrics, such as the maximum value ( $ACCF_{MAX}$ ) of the areal cross correlation function. Case studies were performed on consecutively manufactured tools, such as gun barrels and breech faces, to demonstrate that, even in this worst case scenario, all the tested tools imparted unique surface topographies that were identifiable. These studies provide scientific support for toolmark evidence admissibility in criminal court cases.

Keywords: toolmarks, cross correlation function, forensics

## 1. Introduction

Advances in product requirements and manufacturing have stimulated innovations in the measurement and characterization of surface texture. Standards such as ASME B46.1 [1], ISO 5436 [2] and ISO 25178 [3] define many parameters and associated measurement procedures to characterize aspects of surface texture that are important for functional requirements of industrial components. In the past decade, the Surface and Nanostructure Metrology Group at

the National Institute of Standards and Technology (NIST) has applied its expertise in dimensional surface metrology to improve forensic toolmark identification<sup>3</sup>.

Toolmarks are created when a hard surface, the tool, comes into contact with a softer surface and causes plastic

<sup>3</sup> Certain commercial equipment, instruments, or materials are identified in this paper in order to adequately specify the experimental procedure. Such identification is not intended to imply recommendation or endorsement by the National Institute of Standards and Technology, nor is it intended to imply that the materials or equipment identified are necessarily the best available for the purpose.

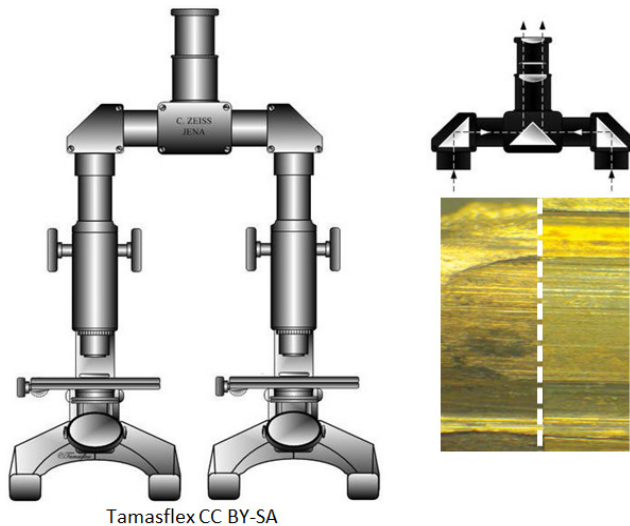


**Figure 1.** A comparison microscope consists of two standard optical microscopes connected with an optical bridge that allows the user to view two images at once side by side. The image on the right shows what an examiner would see when using this instrument [4]. The white dotted line separates the two fields of view. Samples can be translated and rotated independently from one another to find the optimal matching position [5].

deformation. Toolmarks are commonly found on fired bullets and cartridge cases. Toolmarks can be used to link an evidence bullet or cartridge case to a specific firearm (tool), which can lead to a criminal conviction. In the United States, toolmark evidence has been used for over 100 years [4]. At first, examiners relied on visual memory or manual alignment of surface micrographs to make an identification. The invention of the comparison microscope in the 1920s (figure 1) significantly improved this laborious process by giving the examiner the ability to view two surfaces simultaneously under magnification.

Aside from improved optics, automation and digital imaging, very little has changed in the methodology for forensic identification. Data analysis and firearms identification have improved through the development of a nationwide set of regional databases of digitized images, the National Integrated Ballistics Information Network, and associated correlation software, which provides a (proprietary) quantitative estimate of the most likely matches. In 2009, the National Academies published a report, ‘Strengthening Forensic Science in the United States: A Path Forward [6]’, that called into question, among other issues, the objectivity of visual toolmark identification by firearms examiners. The report recommended the development of a precisely specified and scientifically justified protocol that leads to results with well-characterized confidence limits. In the United States, the admissibility of scientific expert testimony, such as that by a firearms examiner, is governed by the Daubert rule [7], which requires a judge to ensure that the expert evidence or testimony in a trial is the product of sound ‘scientific methodology’ derived from a scientific method. Criteria for evidence acceptability include the testability of the scientific principle serving as the basis for the evidence, a known or potential error rate, and the existence and

maintenance of standards of control. NIST developed the Standard Reference Material SRM 2460 standard bullet [8] and SRM 2461 standard cartridge case [9] to facilitate the quality control and traceability of identifications performed in crime laboratories. This paper describes work at NIST to improve the objectivity of toolmark evidence through measurement of areal surface topography, instead of optical contrast, and the application of unambiguous similarity metrics, such as the maximum value ( $ACCF_{MAX}$ ) of the areal cross correlation function.

## 2. Toolmarks

A toolmark results from the contact of two surfaces, the harder of which is defined as the tool. For example, the tool surface of the hard gun barrel interior leaves toolmarks on the softer metal of the fired bullet. Toolmarks are classified as either striated or impressed. Striated toolmarks are created when the tool is dragged across a surface, resulting in a surface topography that has the appearance of parallel lines, called striae. Impressed toolmarks are created when the tool impacts or presses against the surface, resulting in a surface topography that is a negative copy of the tool surface topography. In firearms identification, striated toolmarks are found on bullets while impressed toolmarks are found on cartridge cases. For there to be a potential for toolmark identification, the tool working surface must have individuality and the toolmarks must be reproducible for comparisons [4]. In general, toolmarks have so-called class characteristics, which are common to certain brands or types of tools, and individual characteristics, arising from random variations in tool manufacturing and tool wear. The latter form the basis for the unique identification of a tool. A complication arises from the possible presence of sub-class characteristics, which are common to a relatively small number of sequentially manufactured tools. Experienced firearms examiners are aware that the relatively coarse class and sub-class characteristics cannot be used as a basis for a unique identification.

### 2.1. Bullet—striated toolmarks

Rifled gun barrels have been in existence since the 1800s. The helical lands fabricated in the barrel bore (figure 2) impart a spin on the bullet as it leaves the gun, increasing accuracy and range. The lands are fabricated using different techniques, such as gang broaching, button swaging and hammer forging [4]. These fabrication processes impart unique, microscopic, surface features on the working surface of the gun barrel due to random variations in manufacturing process conditions, tool geometry and wear, burrs and metal chips. These individual characteristics are then imparted onto the soft surface of a bullet as it travels through the barrel (figure 3). A trained firearms examiner can use the resulting striated toolmarks on a recovered bullet to identify the gun that fired it through comparison with a test bullet fired from the same gun.

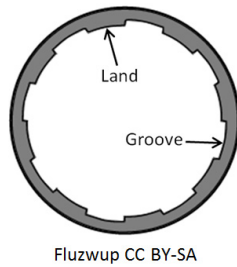


**Figure 2.** Land and grooves of a rifled barrel [10].

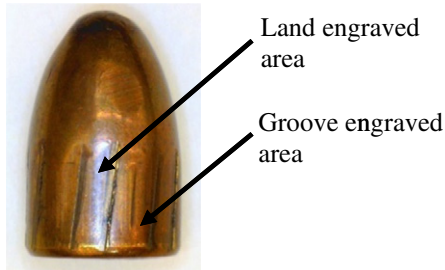


**Figure 3.** A fired bullet with striated tool marks.

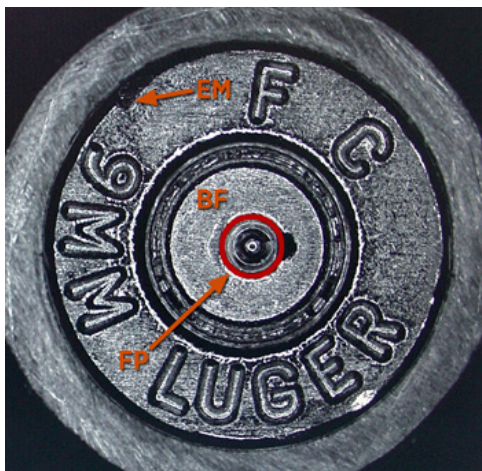
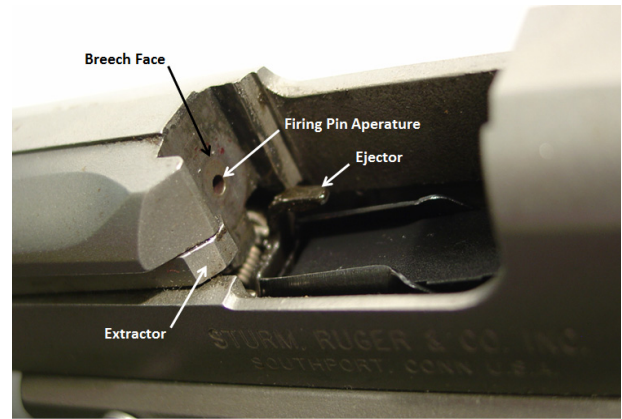


**Figure 4.** Three regions of interest on a fired cartridge case: the breech face impression (BF), the firing pin impression (FP) and the ejector mark (EM) [11].

## 2.2. Cartridge case—impressed toolmarks

Fired cartridge cases are often left at a shooting scene. They typically have three distinct surface areas with impressed toolmarks from the firearm mechanisms (figure 4). The three regions of interest are breechface impressions, firing pin impressions and ejector marks. Figure 5 shows the particular gun components that create these three identifiable toolmarks on the cartridge case.

**2.2.1. Breech face.** This is the flat surface that the cartridge case rests against. When the gunpowder is ignited, the explosive force pushes the cartridge case against the breech face. The surface topography of the breech face is then impressed onto the soft cartridge surface.



Courtesy of Robert Thompson - NIST

**Figure 5.** The ejection port of a semi-automatic pistol showing components that can create the BF and EM marks seen in figure 4. The firing pin is hidden behind the firing pin aperture.

**2.2.2. Firing pin.** When the trigger is pulled, a spring loaded metal pin shoots through an aperture on the breech face and impacts the cartridge primer. This impact causes the primer to ignite which fires the bullet. The impact of the firing pin causes its surface topography to be imparted onto the soft primer surface.

**2.2.3. Ejector mark.** To eject the spent cartridge case out of the gun, the case is pulled back by the pistol extractor. The ejector then impacts the rear edge of the cartridge case where it imparts its surface topography onto the case surface.

## 3. Measurement

Direct measurement of surface topography is a promising avenue to enhance the quality of information obtained from toolmarks [12]. The current practice of optical reflectance microscopy produces images representing optical contrast variations that provide only an indirect measure of surface topography through slope variations and shadowing. The images obtained are affected by lighting conditions, multiple reflections, exposure settings and variations in surface reflectivity (including colour) [13]. The measured topographies presented in this paper were obtained using a disc scanning confocal microscope. The measurement parameters used for various toolmarks are listed below.

### 3.1. Bullet measurement

Due to the striated nature of bullet toolmarks, the feature of interest is the surface height profile of a land impression in a cross section that is approximately perpendicular to the bullet axis. An example of measured topography data obtained from one of our SRM bullets is shown in figure 6. The measurements were performed at the base of the bullet using a  $50\times$  objective with a numerical aperture (NA) of 0.80. The field of view for this objective is  $320\ \mu\text{m} \times 320\ \mu\text{m}$ . For each land, images were stitched, typically with a 25% overlap, resulting in a total measurement area of approximately  $2200\ \mu\text{m} \times 320\ \mu\text{m}$ . The resulting surface height data has a

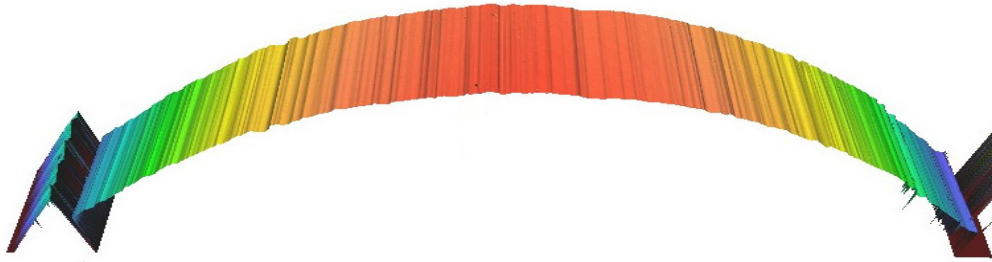


**Figure 6.** 3D topography measurement of a single bullet land of the SRM2460 Standard Bullet.

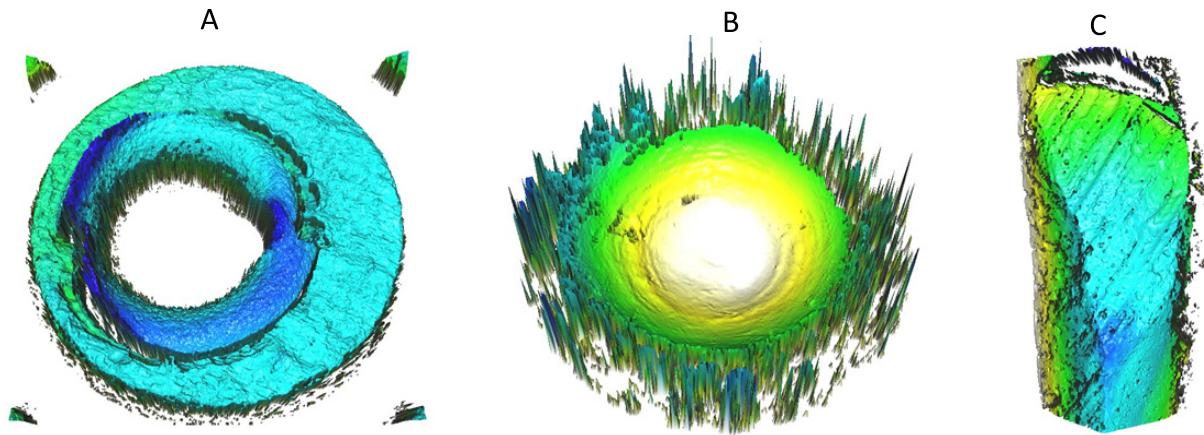


**Figure 7.** 3D topography measurements of the three regions of interest on a cartridge case. (A) Breech face impression, (B) firing pin impression and (C) ejector mark.

sampling interval ('pixel' distance) of  $0.625 \mu\text{m}$  and a vertical resolution of about  $3 \text{ nm}$ . During the measurements, the optical axis of the microscope is aligned perpendicular to the centre of each land. No rotations were performed during the land measurement.

### 3.2. Cartridge case measurement

**3.2.1. Breech face impression.** Measurements were performed using a  $10\times$  objective with an NA of 0.30. The field of view for this objective is  $1.6 \text{ mm} \times 1.6 \text{ mm}$ . To cover the entire breech face,  $3 \times 3$  images were stitched, resulting in a total measurement area of approximately  $4.5 \text{ mm} \times 4.5 \text{ mm}$  with a pixel distance of  $3.125 \mu\text{m}$ . An example of the measured data is shown in figure 7(a).

**3.2.2. Firing pin impression.** Measurements were performed using a  $20\times$  objective with an NA of 0.60. The field of view for this objective is  $800 \mu\text{m} \times 800 \mu\text{m}$ . Only one image was needed to measure the bottom of the firing pin crater. The pixel distance is  $1.562 \mu\text{m}$ . An example of the measured data is shown in figure 7(b).

**3.2.3. Ejector mark.** Measurements were performed using a  $20\times$  objective with an NA of 0.60. The field of view for this objective is  $800 \mu\text{m} \times 800 \mu\text{m}$ . To cover the entire ejector mark, two images were stitched, resulting in a total measurement area of approximately  $800 \mu\text{m} \times 1400 \mu\text{m}$  with a pixel distance of  $1.562 \mu\text{m}$ . An example of the measured data is shown in figure 7(c).

## 4. Metrics for topography similarity

The most commonly used similarity metric for two sets of surface height data,  $Z_A(x, y)$  and  $Z_B(x, y)$ , is the maximum value  $\text{ACCF}_{\text{MAX}}$  of the normalized area cross correlation function. In 2000, NIST proposed the  $\text{ACCF}_{\text{MAX}}$  value, and its equivalent  $\text{CCF}_{\text{MAX}}$  for profile data, to quantify the similarity of three-dimensional (3D) topographies and two-dimensional (2D) profiles for ballistics identification of bullets and cartridge cases [13]. The  $\text{ACCF}_{\text{MAX}}$  value is defined as

$$\text{ACCF}_{\text{MAX}} = \frac{\sum_{i,j} (Z_A(i, j) - \bar{Z}_A) (Z_B(i, j) - \bar{Z}_B)}{\sqrt{\sum_{i,j} (Z_A(i, j) - \bar{Z}_A)^2} \sqrt{\sum_{i,j} (Z_B(i, j) - \bar{Z}_B)^2}}, \quad (1)$$

where the summations and averages  $\bar{Z}$  are performed over points common to both data sets, after translating and rotating one of the data sets such that the value in equation (1) is maximized. The  $\text{ACCF}_{\text{MAX}}$  value, in essence the normalized maximum covariance, varies between  $-1$  and  $1$  irrespective of the bias and variance of the surface height data, although it is undefined for perfectly flat surfaces. An  $\text{ACCF}_{\text{MAX}}$  value of  $1$  (100%) indicates that both surfaces are the same, except for a possible scale factor, whereas an  $\text{ACCF}_{\text{MAX}}$  value of  $0$  corresponds to two uncorrelated surfaces. Due to the applied normalization, the  $\text{ACCF}_{\text{MAX}}$  value is not affected by a different scaling factor in the compared surface heights. Although this insensitivity may be advantageous

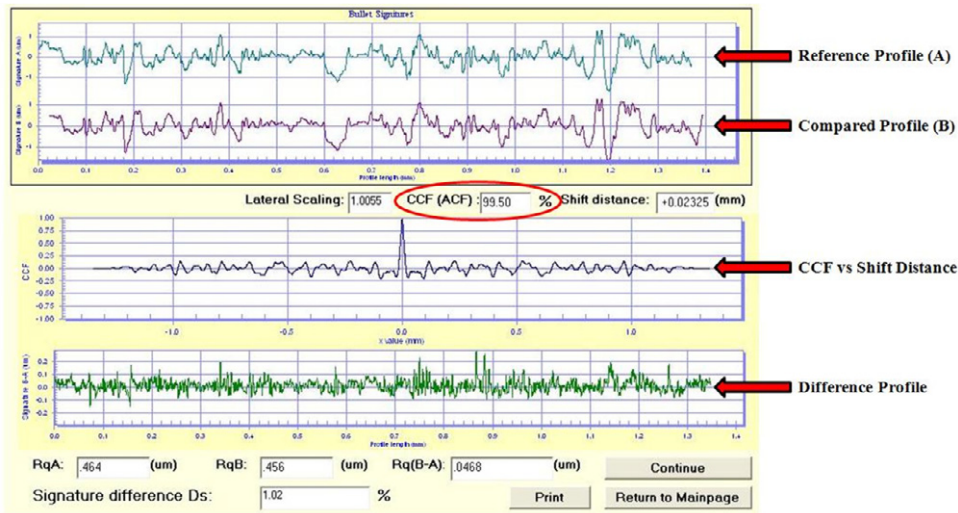


Figure 8. NIST 2D profile correlation program result for two profiles taken from two units of SRM2460.

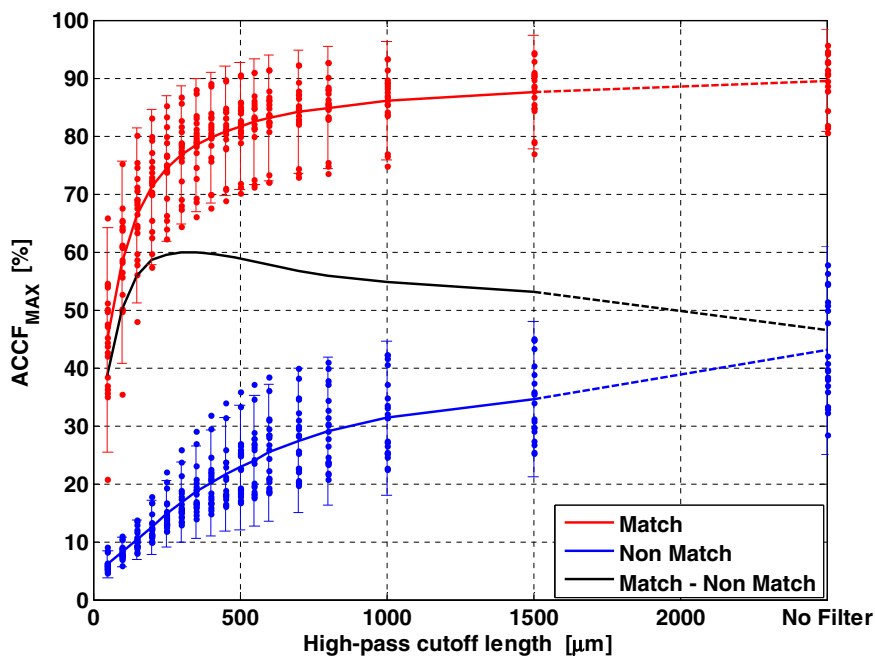


Figure 9. Effect of the high-pass filter cutoff length on the  $ACCF_{MAX}$  of 20 matching and 20 non-matching breechface impression comparisons for a set of cartridge cases fired from consecutively manufactured pistol slides. The intervals represent  $\pm 2$  standard deviations.

when comparing image contrast data, where the scale factor is affected by experimental settings, it does not yield a complete metric for topography similarity. Therefore, NIST also uses a complementary metric, the relative topography difference,  $D_s$ , which is sensitive to scale differences [13]

$$D_s = \frac{\sum_{i,j} ((Z_A(i,j) - \bar{Z}_A) - (Z_B(i,j) - \bar{Z}_B))^2}{\sum_{i,j} (Z_A(i,j) - \bar{Z}_A)^2} \quad (2)$$

It should be noted that both parameters represent an un-weighted areal ‘average’ of surface similarity. This may,

for example, cause performance degradation for surfaces with areas that do not have distinct toolmarks or it may produce noisy measurements of surfaces with areas that have a low variance of surface heights. Furthermore, the parameters do not distinguish between the height variations of interest (i.e. those that represent individual toolmark characteristics) and other height variations, such as those due to (sub-) class toolmark characteristics or due to variations in surface form incurred before or after a gun is fired. These characteristics heighten the importance of proper pre-processing of the data sets, especially masking and filtering. To address these

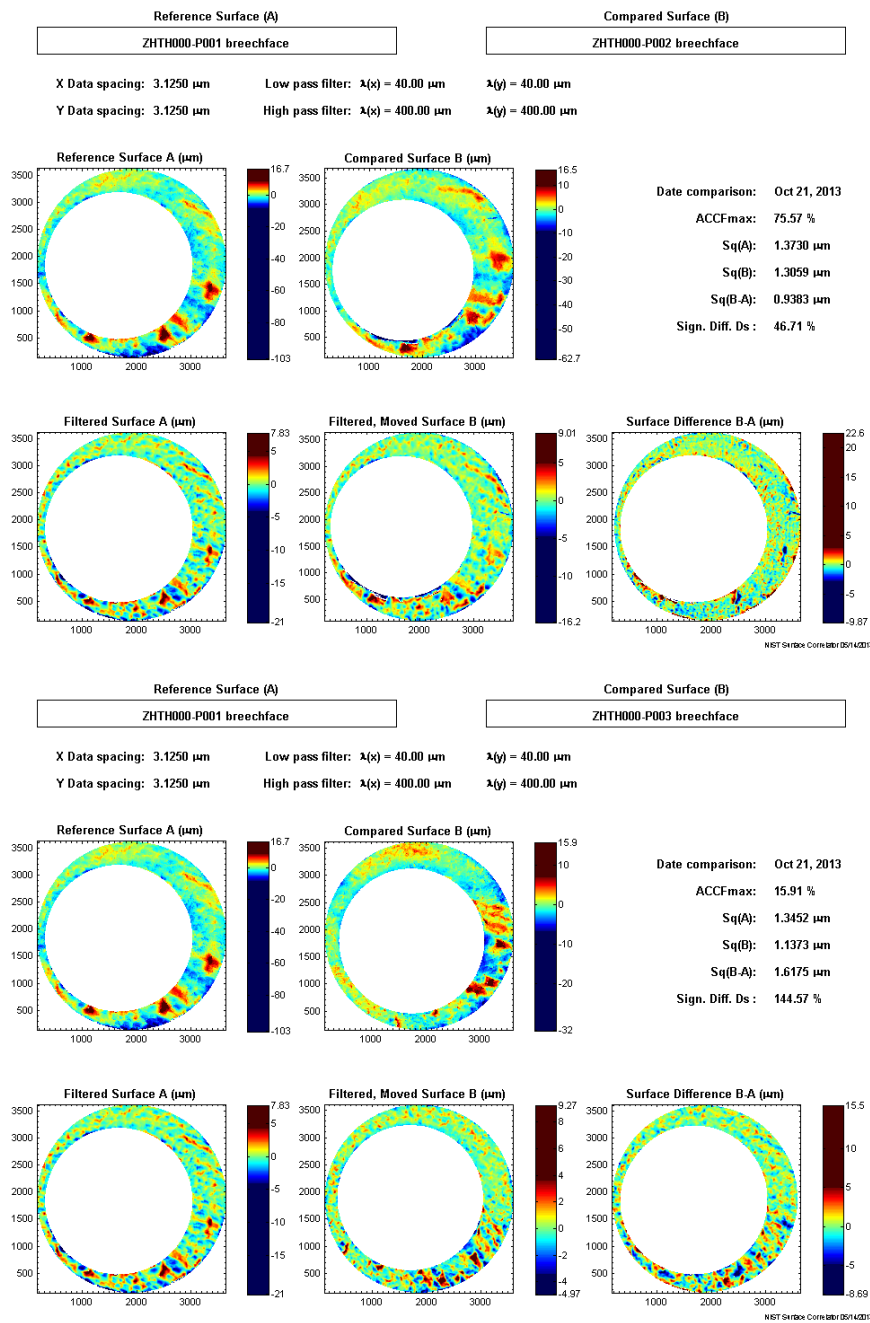


**Figure 10.** Results from the NIST 3D areal topography correlation program. The top image shows the correlation results for breech face impressions from two matching test fires from the Fadul study [17]. The bottom image shows a non-matching correlation.

concerns, NIST is developing other similarity metrics, such as those based on correlation cells [14].

## 5. Data analysis

### 5.1. Bullets

Due to the striated nature of bullet toolmarks, the feature of interest is the surface height profile of a land impression in a cross section perpendicular to the bullet land. Before extracting the profile, the data described in section 3.1 is pre-processed. First, dropouts (i.e. points where no height data was obtained) and outliers (i.e. points where the measured

height is inconsistent with that of neighbouring points) are identified and masked. These dropouts and outliers typically occur in areas with high local slopes. After removing a best-fit circular profile, a band pass Gaussian regression filter is applied to remove low frequency form errors and high frequency noise. Typical filter parameters are a cutoff length of  $2.5 \mu\text{m}$  for the low-pass filter and  $0.25 \text{ mm}$  for the high-pass filter. In principle, the processed data set contains several profiles that can be averaged. There are, however, several challenges to this, including: (i) the profiles are shifted relative to each other due to the land twist angle; and (ii) some areas may have weak or non-existent striations, which impact the average. Therefore, we apply an edge detection

algorithm to identify areas with strong striations and rotate the dataset such that the striations are vertical [15]. The profile is then obtained as the average of profile sections with strong striations. Figure 8 shows the comparison of surface profiles taken from two different SRM2460 standard bullets [8].

## 5.2. Cartridge cases

Due to the areal non-uniformity of impression toolmarks, correlations are performed on the 3D areal topography. First, the data described in section 3.2 is pre-processed. Dropouts and outliers are identified and masked; after which, a best-fit plane or second order surface is removed from the data [12]. Gaussian regression filters are applied to remove low frequency form errors and high frequency noise. The respective filter parameters are chosen to highlight the contribution of individual toolmark characteristics, with a typical high-pass cutoff length on the order of one tenth the area size. Figure 9 shows a high-pass filter parameter optimization study we have performed for cartridge cases [17] fired using consecutively manufactured pistol slides. The filter parameter that yields the highest separation between the distributions of matching and non-matching cases was chosen for the filtering of breech face impression topographies. In this study, that cutoff length is approximately  $400\ \mu\text{m}$ .

It is challenging to estimate the relative position and orientation of two compared surfaces that maximizes the areal cross correlation function between them. We use a combination of global coarse alignment optimization using Fourier transform methods, which is followed by direct local optimization of the objective function to achieve sub-pixel alignment accuracies. Figure 10 shows the correlation results for a known match (top) and a known non-match (bottom) correlation of breech face impressions. The top row of each correlation (reference surface A and compared surface B) represents the trimmed and levelled topographies. The bottom row shows the filtered topographies with filtered surface B in a registered position with respect to filtered surface A. This is the position in which the maximum value of the areal cross correlation function is calculated.

## 6. Case studies

To test the validity of toolmark identifications for firearms, objective statistically based studies are needed. To have a purely objective study, all identifications/exclusions need to be made by a computer without human judgement. One of the most difficult challenges for a toolmark examiner is to distinguish between toolmarks that were made from consecutively manufactured tools. These tools have the highest probability of containing similar marks due to the manufacturing process (i.e. sub-class characteristics), potentially leading to a false identification. These types of toolmarks are often provided to examiners for proficiency testing and training.

The two case studies presented below are based on bullets or cartridge cases fired from consecutively manufactured firearm components. Each study contains a set of known

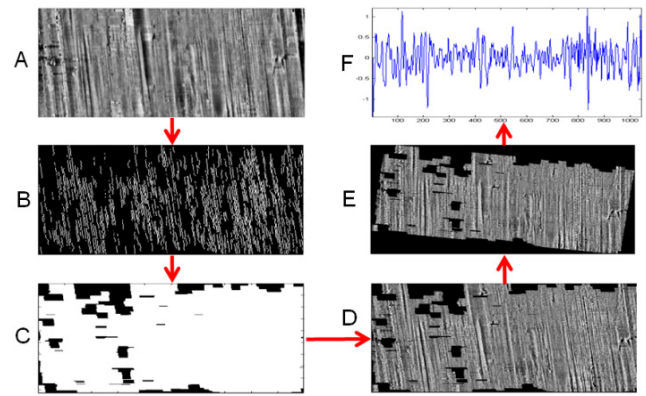


**Figure 11.** Processing steps for bullet land topography: (A) remove cylindrical form and filter; (B) apply Canny edge detection to detect striae; (C) create mask for areas with weak striae; (D) mask out areas with weak striae; (E) rotate image to align profiles; and (F) average data into a single profile.

test fires and a set of unknown test fires. We measured the surface topography of each sample using a disc scanning confocal microscope and calculated the similarity metric for every pair wise comparison in each study. In both studies, we observed a statistically significant separation between the distributions of the similarity metric for the matching and non-matching samples. As a first approach, we established the identification baseline value for the similarity metric as the mean of its distribution for comparisons of known matching samples minus three times the standard deviation. For the observed separation between the matching and non-matching distributions, this approach is relatively conservative; that is, it is expected to have a relatively low false identification probability, which, from a legal perspective, represents the most critical error rate. A practical challenge is that the distribution for the known matches is usually based on fewer comparisons than that of the known non-matches, with an associated increase in distribution uncertainty.

### 6.1. Bullets fired from ten consecutively rifled 9 mm Ruger pistol barrels

Our study used bullets from an international comparison led by Hamby [16] involving ten consecutively rifled barrels from a single manufacturer. Each barrel fired two bullets to create a set of 20 known bullets. The barrels were then randomized and used to fire a set of 15 unknown bullets. The study was designed to be a blind test. For each unknown bullet, the participants were tasked to identify the corresponding barrel by comparing the bullet with bullets from the known set. To evaluate application of the  $CCF_{MAX}$  similarity metric for objective identification, NIST measured the topography of the land impressions of each bullet with a disc scanning confocal microscope. After removing the cylindrical form component and filtering, a Canny edge detector algorithm was applied to estimate the orientation of the striae (land twist angle) and to identify areas with strong striations (figure 11). The profiles corresponding to areas with strong striations were then averaged into a single profile for correlations. More details on the processing steps can be found in [15].

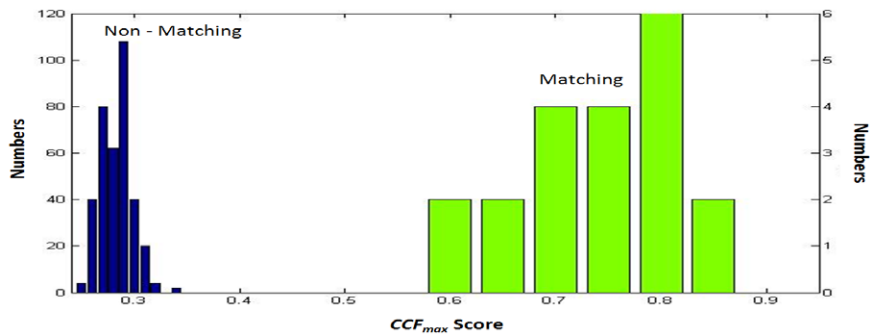


**Figure 12.** Distribution of the  $CCF_{MAX}$  values for the known matching and known non-matching sample comparisons of 20 bullets fired from ten consecutively rifled barrels.

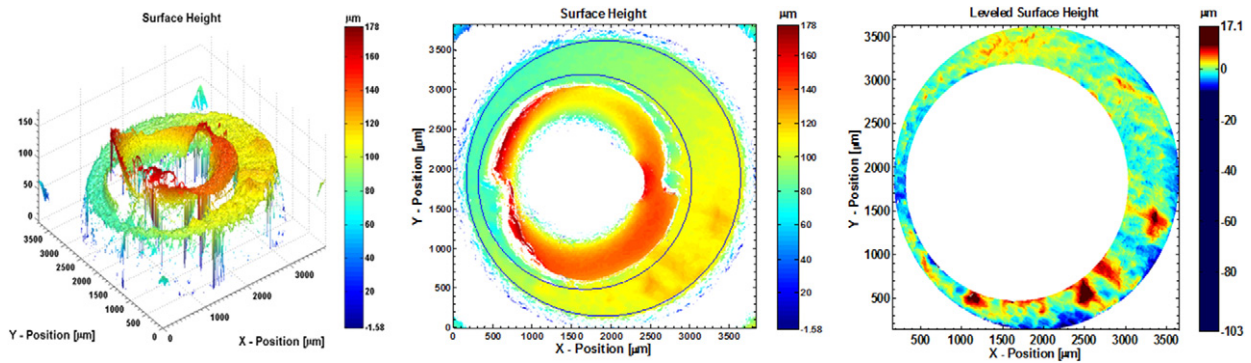


**Figure 13.** Left: raw measurement data. Middle: raw data with trim boundaries. Right: trimmed and leveled data.

Comparing the bullet profiles of the known set has yielded distributions for the known matching and known non-matching  $CCF_{MAX}$  values (figure 12). The matching distribution was then used to establish the  $CCF_{MAX}$  baseline identification value. Any  $CCF_{MAX}$  value above the baseline was considered to be an identification while anything below was considered to be an exclusion. Based on this criterion, there were no false identifications or false exclusions in the known comparisons. The unknown bullet profiles were then correlated against the profiles of every bullet in the known set. Using the  $CCF_{MAX}$  metric and its baseline value, all 15 unknown bullets were correctly identified back to the barrel that fired them. There were no false identifications or exclusions for all 30 matching and all 270 non-matching sample comparisons.

**6.2. Cartridge cases fired from ten consecutively manufactured 9 mm**

This study used cartridge cases from a study by Fadul *et al* [17] involving ten consecutively manufactured pistol slides. Each slide was used to fire two cartridge cases creating a set of 20 known cases. The slides were then randomized and were used to fire a set of 15 unknown cases. After over 400 firings, another five unknown cartridge cases were collected (persistence testing) to yield a total of 20 unknown cartridge cases. To evaluate application of the  $ACCF_{MAX}$  metric for objective identification, NIST measured the topography of the breech face impression of every test fire with a disc

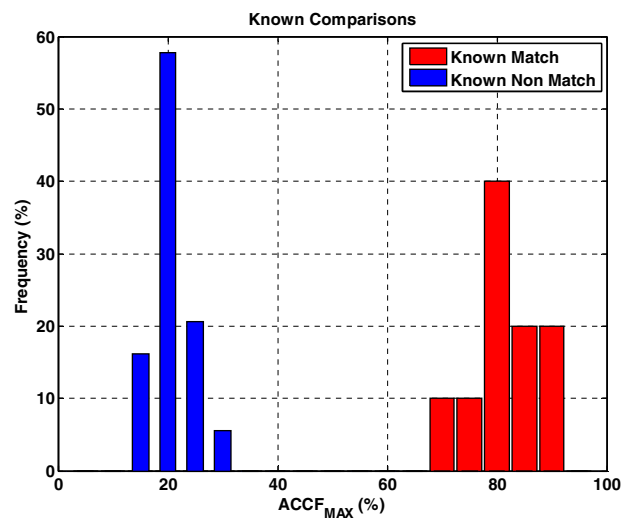


**Figure 14.** Distribution of the  $ACCF_{MAX}$  values for the known matching and known non-matching sample comparisons of the breech face impression of 20 cartridge cases fired from ten consecutively manufactured pistol slides.

scanning confocal microscope. A mask was applied to the raw topography data to remove the primer blow back area [4] and the edges of the breech face impression (figure 13). The trimmed data set was then processed for correlation as discussed in section 5.2. Examples of the correlation results can be seen in figure 10.

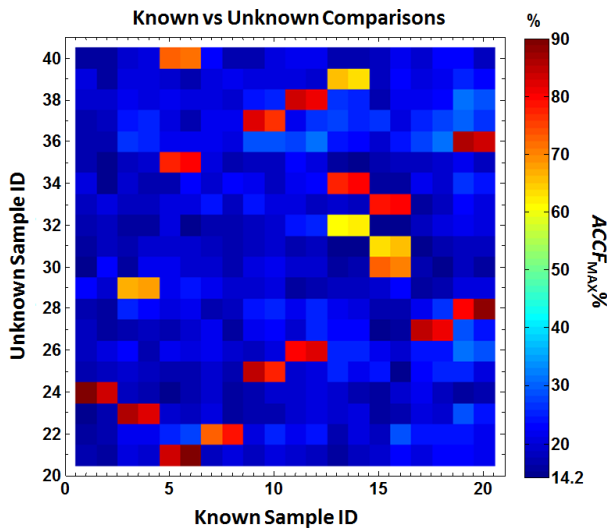


**Figure 15.** Correlation matrix representing the  $ACCF_{MAX}$  values for all 400 comparisons of a known breech face impression sample with an unknown sample.

Pairwise comparison of the surface topography data of the 20 known samples yielded the distributions for the known matching and known non-matching  $ACCF_{MAX}$  values (figure 14). The matching distribution was then used to establish the  $ACCF_{MAX}$  baseline identification value. Any  $ACCF_{MAX}$  value above the baseline was considered to be an identification while anything below was considered to be an exclusion. Based on this criterion, there were no false identifications or false exclusions in the known comparisons. The correlation matrix of figure 15 shows the  $ACCF_{MAX}$  values for all 400 comparisons of a known cartridge case with an unknown cartridge case. Application of the  $ACCF_{MAX}$  metric and its baseline value yielded no false identifications or exclusions for all 40 matching comparisons and all 360 non-matching comparisons.

## 7. Discussion

For two challenging scenarios of consecutively manufactured firearm components, the  $CCF_{MAX}$  and  $ACCF_{MAX}$  similarity metrics, as applied to surface topography data, yielded significant separation between the distributions of the similarity metric for matching and non-matching samples. The metrics were successfully applied to automatically identify the specific firearm that fired a bullet or cartridge case from a pool of consecutively manufactured firearms. Similarity metrics based on measured surface topography yield a higher level of objectivity than metrics obtained using reflectance microscopy because the measurand is clearly defined and is less affected by experimental settings. Furthermore, there is a mature infrastructure for surface topography metrology that facilitates the quality control and traceability of the measurements, enabling comparisons of data obtained at different labs using different instruments.

The similarity parameters represent an areal ‘average’ of surface similarity and do not distinguish between the height variations of interest (i.e. those that represent individual toolmark characteristics) and other height variations

(i.e. sub-class characteristics and unmarked areas). To address these concerns, NIST is developing other similarity metrics, such as those based on the number of valid correlation cells [14], which address both the similarity and areal distribution consistency of surface patches with common features. This approach also holds promise to facilitate the estimation of error rates; that is, the probability that a determination of a match is incorrect (false identification) or the probability that a determination of a non-match is incorrect (false exclusion). The current lack of well-characterized confidence limits is one of the key concerns identified in the NAS report [6]. Extensive validation of proposed similarity metrics and analysis procedures, including error rate estimation, is required before they can contribute to a toolmark examiner’s testimony in court. NIST is developing an open research database of toolmark topography data for challenging identification scenarios, such as those posed by consecutively manufactured tools, which will aid the development and validation of toolmark identification metrics and protocols.

## References

- [1] ASME B46.1 2009 *Surface Texture (Surface Roughness, Waviness, and Lay)* (New York: American Society of Mechanical Engineers)
- [2] ISO 5436 2000 Geometrical product specifications (GPS)—surface texture: profile method *Measurement Standards* (Geneva: International Organization for Standardization)
- [3] ISO 25178 2010 *Geometrical Product Specifications (GPS)—Surface Texture: Areal* (Geneva: International Organization for Standardization)
- [4] Thompson R 2008 Firearm identification in the forensic laboratory *National District Attorney’s Association NIJ Grant 2008-MU-MU-K004*
- [5] Tamasflex 2013 Comparison microscope, available from: [http://en.wikipedia.org/wiki/Comparison\\_microscope](http://en.wikipedia.org/wiki/Comparison_microscope)
- [6] National Research Council 2009 *Strengthening Forensic Science in the United States: A Path Forward* (Washington DC: The National Academies Press)
- [7] Daubert v Merrell Dow Pharmaceuticals, Inc. 1993 509 US 579, 589
- [8] NIST SRM Certificate 2012 *Standard Reference Material®2460 Standard Bullet* available from: [www-s.nist.gov/srmors/view\\_detail.cfm?srm=2460](http://www-s.nist.gov/srmors/view_detail.cfm?srm=2460)
- [9] NIST SRM Certificate 2012 *Standard Reference Material®2461 Standard Cartridge Case* available from: [www-s.nist.gov/srmors/view\\_detail.cfm?srm=2461](http://www-s.nist.gov/srmors/view_detail.cfm?srm=2461)
- [10] Fluzwup 2013 Rifling, available from: <http://en.wikipedia.org/wiki/Rifling>
- [11] Zheng X A 2012 Standard bullets and casings, available from: [www.nist.gov/pml/div683/grp02/sbc.cfm](http://www.nist.gov/pml/div683/grp02/sbc.cfm)
- [12] Vorburger T V *et al* 2007 Surface topography analysis for a feasibility assessment of a National Ballistics Imaging Database *NIST Interagency Report NISTIR 7362* (Gaithersburg, MD: National Institute of Standards and Technology)
- [13] Song J and Vorburger T V 2000 Proposed bullet signature comparisons using autocorrelation functions *Proc. 2000 NCSL* (Toronto: National Conference of Standards Laboratories International)
- [14] Song J 2013 Proposed ‘NIST Ballistics Identification System (NBIS)’ based on 3D topography measurements on correlation cells *AFTE J.* **45** 184–94

- [15] Chu W, Song J, Vorburger T, Thompson R and Silver R 2011 Selecting valid correlation areas for automated bullet identification system based on striation detection *J. Res. Natl Inst. Stand. Technol.* **116** 647–53
- [16] Hamby J 2009 The identification of bullets fired from 10 consecutively rifled 9 mm Ruger pistol barrels: a research project involving 507 participants from 20 countries *AFTE J.* **41** 99–110
- [17] Fadul T, Hernandez G, Stoiloff S and Gulati S 2011 An empirical study to improve the scientific foundation of forensic firearm and tool mark identification utilizing 10 consecutively manufactured slides *NCJRS Grant Final Report* 237960